Arabian Journal of Chemistry (2022) **15**, 104299

King Saud University

Arabian Journal of Chemistry

www.ksu.edu.sa
www.sciencedirect.com

ORIGINAL ARTICLE

Anticancer potential of novel 5-Fluorouracil co-crystals against MCF7 breast and SW480 colon cancer cell lines along with docking studies

Farhat Jubeen [a], Sana Ijaz [a], Ishrat Jabeen [b], Usman Aftab [c], Wajeeha Mehdi [b], Awais Altaf [d,*], Siham A. Alissa [e], Hanan A. Al-Ghulikah [e], Safa Ezzine [f,g], Imen Bejaoui [h], Munawar Iqbal [i,*]

[a] *Department of Chemistry, Government College Women University Faisalabad, Pakistan*
[b] *School of Interdisciplinary Engineering and Sciences (SINES), National University of Sciences and Technology (NUST), 44000, Sector H12, Islamabad, Pakistan*
[c] *Department of Pharmacology, University of Health Sciences, Lahore, Pakistan*
[d] *Institute of Molecular Biology and Biotechnology, Centre for Research in Molecular Medicine, The University of Lahore, Lahore 53700, Pakistan*
[e] *Department of Chemistry, College of Science, Princess Nourah bint Abdulrahman University, P.O. Box 84428, Riyadh 11671, Saudi Arabia*
[f] *Department of Chemistry, College of Sciences, King Khalid University, P.O. Box 9004, Abha 61413, Saudi Arabia*
[g] *Laboratoire des Matériaux et de L'Environnement Pour le Développement Durable LR18ES10, 9 Avenue Dr. Zoheir Sai, Tunis 1006, Tunisia*
[h] *Department of Chemistry, College of Arts and Science, Sarat Abidah, King Khalid University, Saudi Arabia*
[i] *Department of Chemistry, Division of Science and Technology, University of Education, Lahore, Pakistan*

Received 5 July 2022; accepted 20 September 2022
Available online 23 September 2022

KEYWORDS

5-Fluorouracil;
Co-crystals;
Dimers;
Molecular docking;
MTT analysis;
Antitumor efficacy

Abstract In the present investigation, 5-Fluorouracil co-crystals with four cyclic dimers of amino acids (Glycine, Tryptophane, Leucine and Alanine conformers are prepared via co-crystallization route, with an aim to improve its anticancer effectiveness and to minimize its associated drawbacks. The prepared co-crystals were characterized by FTIR and PXRD techniques. FTIR revealed the presence of respective functional groups in the prepared co-crystals. Frequencies (v) of N—H (3416 cm^{-1}) and carbonyl group (1671 cm^{-1}) in the 5-Fu (FTIR) spectrum were considerably moved in all co-crystal's spectra exhibiting the development of new interactions. 5-Fu peak at

* Corresponding authors.
E-mail addresses: awaisaltaf362@yahoo.com (A. Altaf), bosalvee@yahoo.com (M. Iqbal).
Peer review under responsibility of King Saud University.

ELSEVIER Production and hosting by Elsevier

https://doi.org/10.1016/j.arabjc.2022.104299

2θ = 28.48° was visibly transformed in the co-crystal's graphs of PXRD. MTT assays was studied on MCF7 breast and SW480 colon cancer cell lines using 0.78 to 200 μg mL^{-1} dose concentration. Co-crystals with Tryptophane and Leucine cyclic dimers revealed highest potential (99 % and 100 %) respectively, against colon cancer cell line Likewise Alanine and Tryptophane dimers furnished promising efficiency (100 %) against MCF7 cell line Genetic Optimization for Ligand Docking/GOLD was applied to evaluate the latent anti-tumor behaviors against the proteins [C-myc. (PDB ID: 6G6K, Thymidylate synthase (PDB ID:1HVY) and protein kinase (PDB ID: 2X18). Results revealed that the developed 5-Fluorouracil co-crystals have promising antitumor efficacy as compared to already reported 5-Fu co-crystals and 5-Fu alone.

1. Introduction

To date, cancer is the second leading cause of death globally with 9.6 million mortalities reported in the year 2018, which need to tackled by developing new anticancer agents (Ferlay et al., 2019, Al-Anazi et al., 2022, Albratty and Alhazmi 2022, Koparir et al., 2022). Chemotherapy is the widely applied approach in the treatment of cancer (other includes radiotherapy and surgery) but drawbacks of their use have been a concerning issue for researches and efforts are being done to minimize them (Zhang et al., 2018, Pradhan and Vishwakarma 2020). In this regard, chemical modifications of an active therapeutic drug to optimize its desired effects by reducing the drawbacks is the intriguing modern approach. The use of heterocyclic compounds, especially those containing nitrogen is an extensively studied area in the respective field (Benaka Prasad et al., 2018a, Benaka Prasad et al., 2018b, Lang et al., 2020, Raveesha et al., 2022, Vidyavathi et al., 2022). Hence, there is need to synthesize a new bioactive material since the existed compounds efficiency is reduced with the passage of time and this regard various techniques have been applied for the synthesis of organic compounds (Kousar et al., 2015, Khalafallah and Ahmed 2017, Ocheni and Clement 2017, Deeba et al., 2018, Abdellatif and Abd El Rady 2020, Abdellatif and El Rady 2020, Amos-Tautua et al., 2020).

5-Fluorouracil (5-Fu), (Carrillo et al., 2015, Jubeen et al., 2018) was discovered half a century ago, persists to be extensively used in the cure of common malignancies involving colon cancer (Hong et al., 2020), breast (Su et al., 2020) brain (Shinde et al., 2020) and skin (de Oliveira et al., 2020). Even though 5-Fu is the better-quality chemotherapeutic agents for CRC (colorectal cancer) (Vodenkova et al., 2020), still it has some shortcomings that include fast metabolism, very short-term half-life, minimal bioavailability, cell mortality and insufficient selectivity for tumorous cells, all these drawbacks limit its efficacy in cancer chemotherapy (Krishnaiah et al., 2003, Entezar-Almahdi et al., 2020) and the response rate is reported only 10–15 % (Sethy and Kundu 2021). But it is reported in various studies that when 5-Fu is mixed with new anti-tumor drugs, the response ratio are elevated to 40–50 % (Gu et al., 2019). Hence, new therapeutic approaches are of urgent necessity to fight drug endurance and other above-mentioned drawbacks to improve drug response rates.

Numerous approaches for structural modifications of 5-Fu are devised and tested, in this regard. The most profound strategies are following; by derivatization at N1 or N3, or both and by conjugation with macromolecules (Radwan and Alanazi 2014, Kumar et al., 2017), by DNA intercalation (Zhou et al., 2013, Sanduja et al., 2020) and designing of 5-Fu loaded nanoparticles to increase the efficiency by increasing the surface area. Among all methods mentioned above, no strategy presents green synthesis, no need of purification and seclusion of the end product.

There is an innovative approach called co-crystallization that comprises all the above-described synthesis needs in a distinct approach (Stoler and Warner 2015). Many co-crystals of 5-Fu have been reported in which 5-Fu co-crystals were designed with acridine, phenazine (Delori et al., 2013), piperazine (Moisescu-Goia et al., 2017) urea, thiourea, acetanilide and aspirin (Jubeen et al., 2019) organic acids (Jubeen et al., 2020). All of these containing more electronegative groups in their molecules i.e., N, O, F, which are typically liable for hydrogen bonding interactions. Almost all of these co-crystallization products have despite of their excellent positive effect in improving drug efficiency has some draw backs associated with them that includes, intramolecular hydrogen bonding of solvent used, significance of the co-former was not mentioned, commercial accessibility of some co-formers and transportation of the synthesized drug through plasma and tissue walls.

This study presents the synthesis of novel prodrugs by using Amino acids cyclic dimers as co-formers. Amino acids are commercially accessible and have substantial structural variety. The synthesized prodrugs have lipophilic and hydrophilic characters that ease in transportation through plasma and tissue walls. Negligible use of solvent, in this case, helped to minimize the problems of byproduct formation and separation of the end product to a great extent. The formation of supramolecular interactions was examined via FTIR and structural changes among 5-Fu and co-crystals were assessed by powdered XRD. Moreover, to evaluate effective antitumor prodrugs, *in vitro* biological study of prepared co-crystals and molecular docking were done. Significance of this study lies in evaluation of the activity of prodrugs, which is performed against two cancer cell line via MTT Assay in contrast to previous studies that involve evaluation against one tumor cell line. Molecular Operating Environment/MOE software were used to interpret the interactions between the three target proteins and 5-Fluorouracil which is another significance of this study. In comparison to 5-Fu alone, computational results reveal that new solid formulations offer promising anti-cancer effectiveness. Following the successful manufacture of these co-crystals and the increase of 5-Fu's capacity to suppress cancer cell development, these new co-crystals can be used for *in vivo* study and membrane crossing capacities in future.

2. Material and methods

2.1. Materials

5-Fluorouracil (Sigma-Aldrich, 99 %), and other chemicals used in this study to synthesize targeted co-crystal are Ethanol (Merck KGaA, 99.5 % purity), Acetone (Merck KGaA, 99 %), Glycine (Sigma-Aldrich, 98 %), Leucine (Sigma-Aldrich, 99 %), Alanine (Sigma-Aldrich, 98 %), Tryptophane (Sigma-Aldrich, 98 %), Glycerol (Commercial suppliers,98 %) and Distilled Water (Commercial suppliers, 100 %).

2.2. Conformers synthesis methodology

The synthesis of our desired co-former consists of the following two methods. The first one includes the cyclic dimerization of four distinctive amino acids (Leucine, Alanine, Glycine and

Tryptophane) through fabrication method which reported by (Pokorna et al., 2019). Glycerol (30 ml) was added in a flask of 100 ml equipped with reflux condenser followed by the addition of Glycine (12 g) under constant stirring at 175–180 °C. The reaction mixture was agitated for 50 min. Then, the reaction mixture was cooled at room temperature, distilled with 12 ml distilled water and left in the refrigerator overnight. The obtained crude product (dimer) was filtered, washed with 50 % ethanol and recrystallized to get pure product with 89 % yield of glycine cyclic dimer (Scheme. 1).

Same procedure was performed with all other selected amino acids [Leucine, Alanine and Tryptophane] and yield of these cyclic amino acid dimers were 82 %, 80 % and 85 % respectively. Scheme 2–4.

2.3. Synthesis of targeted co-crystal

After the successful formation of the above four precursors, the desired co-crystal was synthesized by following the non-grinding solution method. The procedure followed here are in accordance with the literature (Yan et al., 2009, Moisescu-Goia et al., 2017). The solution of API (1.25 g) and co-formers [2,5 Diketopiperazine, 1.09 g; 3,6-Dimethyl-2,5-Pipera zinedione, 1.36 g; 2,5-Piperazinedione-3,6-bis-2-methylpropyl, 2.11 g; Cyclo-L-tryptophane-L-tryptophane, 3.55 g] (Scheme 1–4) were separately warmed in 10 ml acetone at 90 °C until a clear solution obtained. The API and each co-former were then taken in equal ratio 4.4 mM into a beaker and reheated for 3 min at 90–100 °C. Solution was left to cool down at room temperature. After cooling, the solutions were enclosed with foil and allowed to slowly evaporate to yield the pure crystal product.

2.4. Characterization

FTIR analysis were performed for both co-former and co-crystal products. ATR-FTIR spectrophotometer with the range of 400–4000 cm^{-1} was used. The spectrum of 5-Fu in comparison to all spectrum of co-crystals was assessed. Mainly the frequencies of amine/—NH and carbonyl —C═O groups were focused to validate the successful synthesis of co-crystal (Moisescu-Goia et al., 2017). Crystallinity was assessed via PXRD. While cytotoxicity was evaluated trough MTT assay against two cancer cell line (Fang et al., 2015, Dai et al., 2016, Petaccia et al., 2016). Computational/Docking study was conducted using GOLD (Genetic Optimization for Ligand Docking) software.

2.5. In-vitro MTT assay

The antitumor assay was done on SW-480 colon and MCF-7 breast cancer cell lines utilizing MTT assay (Aftab and Sajid, 2017; Patil et al., 2020a; Patil et al., 2020b) 96-well plate were used to cultivate the cancer cells in DMEM (Gibco Dulbecco's Modified Eagle Medium) along with 10 % fetal bovine serum and 1 % antibiotics (streptomycin and penicillin-G) for 24 h in humidified conditions at 37 °C in 5 % CO_2.

Trypsinization (Cell dissociation process via trypsin, after adding into cell culture, trypsin breaks proteins that help the cells to adhere the vessel) was performed after the creation of a confluent monolayer of actively dividing cells and cell suspension (10^5 cells/ ml) was planted in the wells containing culture media and varied concentrations (200 µM, 100 µM, 50 µM, 25 µM, 12.5 µM 6.25 µM, 3.12 µM 1.56 µM and 0.78 µM) of the derivatives of 5-Flourouracil. In 5 % CO_2 environment, incubation at 37 °C for two days was done. After measuring cellular viability for each derivative concentration, 20 µl of MTT (5 mg/mL PBS) was added to each well and plates were incubated at 37 °C for 3 h in a 5 percent CO^2 atmosphere. The medium was carefully removed after incubation. To solubilize the formazan crystals, 100 µl of DMSO was added. The optical density (O.D.) of the wells was then measured using a microplate reader at 570 nm with a reference of 655 nm. The IC_{50} was calculated using a dose-dependent curve. To compute the inhibition rate (Percentage of cells which are inhibited/dead after exposure to our compounds) Req. 1 was applied (OD = optical density).

$$Inhibition\ \ rate = \frac{OD_{control\ \ sample} - OD_{treated\ \ sample}}{OD_{control\ \ sample}} \quad (1)$$

2.6. Computational study: 5-Fu-protein interactions study for cancer therapy

2.6.1. Protein selection criteria

The selected proteins should be found in Homo sapiens and supported by literature. Recently published X-ray crystal structures of proteins, i.e., Thymidylate synthase, Akt-3 and CMYC were used for the molecular modelling studies. The target protein to study colorectal cancer was Thymidylate synthase. It is a vital enzyme for DNA duplication and cell development because it is the only source of thymine nucleotide precursors for DNA synthesis (Danenberg et al., 1999; Niedzwiecki et al., 2017). Expression levels of thymidylate synthase have previously been identified as possible indicators in colorectal cancer. Decrease in levels of Thymidylate synthase causes cell death leading to overall subsistence and disease-free survival. This protein is sensitive to 5-Fu. The target protein for breast cancer were Protein Kinase and MYC. AKT (protein kinase) appears as sufficient target for breast cancer (Hinz and Jücker 2019). AKT has isoforms, they are correlated with complete survival and treatment response in an isoform-specific approach. Owing to its oncogenic character, AKT3

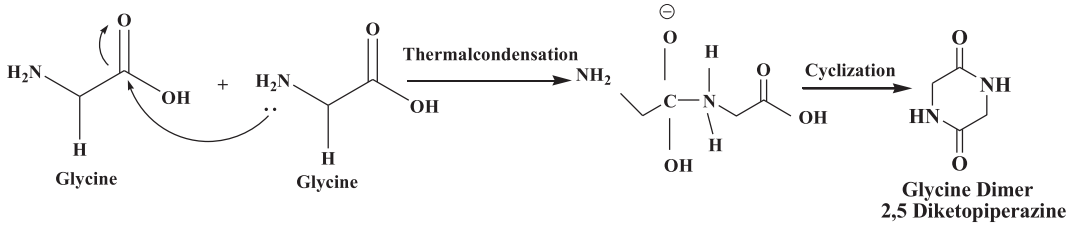

Scheme 1 Synthesis of Glycine cyclic dimer from Glycine mononers.

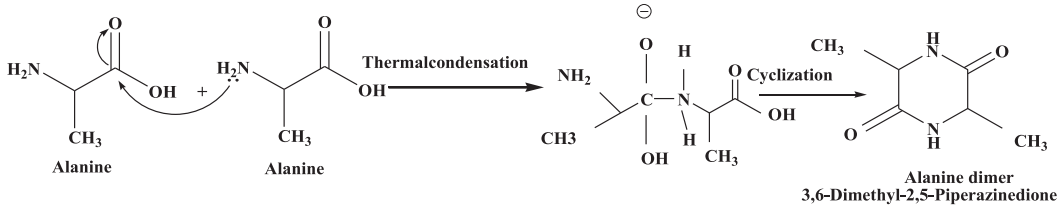

Scheme 2 Synthesis of Alanine cyclic dimer from Alanine mononers.

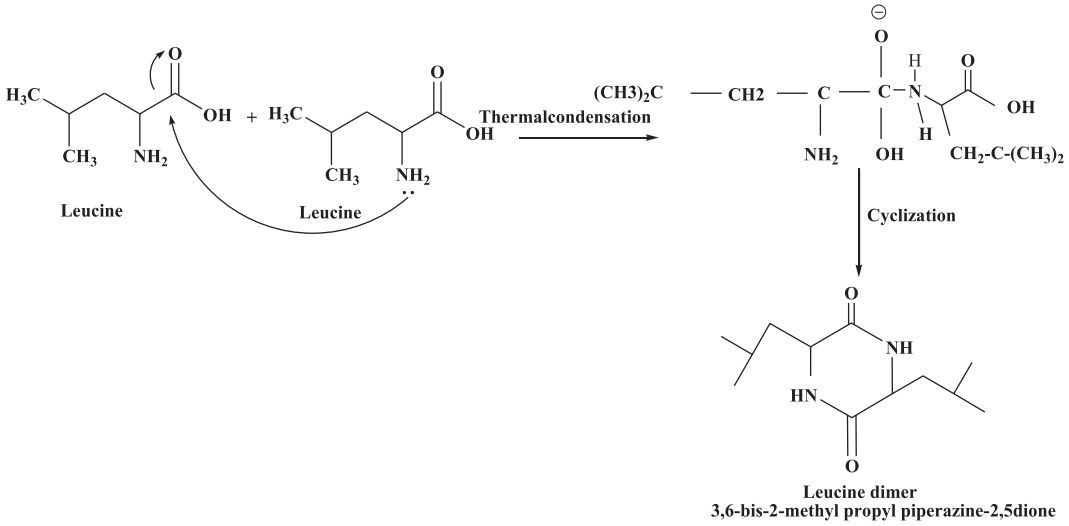

Scheme 3 Synthesis of Leucine cyclic dimer from Leucine mononers.

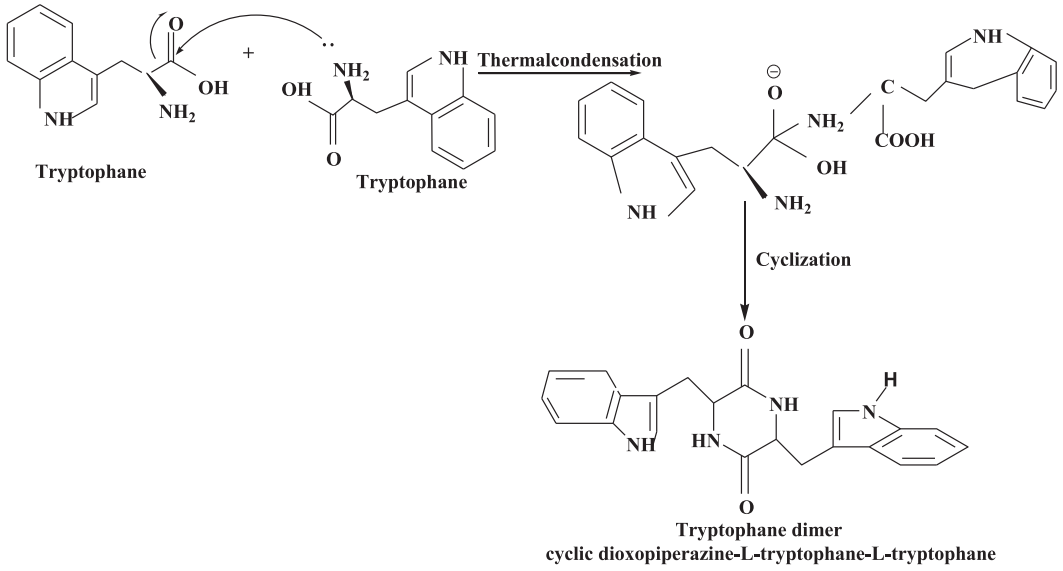

Scheme 4 Synthesis of Tryptophane cyclic dimer from Tryptophane mononers.

was considered. PH domain determines the impact of the isoform-specific inhibitors (Buikhuisen et al., 2021). MYC is overexpressed in most of the aggressive subtype breast cancer. Targeting c-MYC is considered as a potent procedure for anti-tumor therapy(Sammak et al., 2019), (Strippoli et al., 2020) and (Arango et al., 2003).Region considered from the domain

architecture is basic region/helix–loop–helix/ leucine zipper domain since this region mediates and regulates protein–protein interactions (PPIs).

2.6.2. Protein data collection

The protein structures were downloaded from RSCB (Research Collaboratory for Structural Bioinformatics) PBD (Protein Data Bank). A set of three proteins, previously reported for cancer progression were selected for molecular modeling studies. These proteins includes, Thymidylate synthase (PDB ID:1HVY, X-ray resolution of 1.90 Å) (Phan et al., 2001) Akt (PDB ID: 2X18, resolution of 1.46 Å), and c-myc. (PDB ID: 6G6K, resolution of 1.35 Å) (Sammak et al., 2019).

2.6.3. Ligand collection

The 2D structure of the five amino acid dimers; alanine, glycine, leucine and tryptophan, and 5′-Fluorouracil were constructed using ChemDraw software.

2.6.4. Binding pocket identification

Protein's binding pockets were identified using MOE (Molecular Operating Environment) software. Each protein had its own characteristic binding pocket. 5 Å area was selected around co-crystallized ligand for identification of the binding pocket for the potential ligands. Thymidylate synthase (PDB ID: 1HVY) was co-crystallized with dUMP (Deoxyuridine monophosphate), the selected dimensions of the binding pocket were X = 3.0910, Y = 2.7270 and Z = 11.8830. Protein kinase (PDB ID: 2X18) having a co-crystallized ligand EPE (4-(2-hydroxyethyl)-1-piperazine ethanesulfonic acid). The dimension of the binding pocket of protein were X = 23.7100, Y = 93.8179 and Z = 17.6390. The protein's binding pocket of 6G6K was identified with dimensions of X = −60.1, Y = −61.8 and Z = −63.8 around the DNA binding region as reported (Sammak et al., 2019).

2.6.5. Docking protocol

To conduct docking GOLD (Genetic Optimization for Ligand Docking) software. GoldScore function was employed as a scoring function for ligand–protein docking. The following is the GoldScore relation as shown in Eq. (2) (Verdonk et al., 2003).

$$\text{GOLD Fitness} = S_{\text{hb\_ext}} + S_{\text{vdw\_ext}} + S_{\text{hb\_int}} + S_{\text{vdw\_int}} \quad (2)$$

Two steps docking were done and 100 poses per ligand per protein were generated. In the first docking, five amino acid residues were docked into the attachment site of the selected target proteins (cMYC, AKT-3 and Thymidylate synthase). In the second docking, output of first docking was used as an input and it was docked against 5-Fluorouracil. Pose evaluation was conducted on the basis of interactions between amino acid residues and 5-Fluorouracil.

3. Results and discussion

3.1. FTIR analysis

Various vibrational modes of chemical bonds and functional groups take up in the infrared region showed differential absorption peaks. The FTIR spectra of all compounds result in the characteristic absorption peaks which facilitate us to characterize and identifies the corresponding compound.

3.1.1. FTIR analysis of amino acid monomer and dimer

The most distinctive peak in amino acid monomers is due to the stretching the —NH bond appeared at 3300–3000 cm^{-1}. The bending vibration of —NH group in primary amines is detected in the region of 1650–1580 cm^{-1}. This peak was found to be precise and close to the carbonyl region. Amines is examined in the region 910–665 cm^{-1} with broad peak due to —NH wagging motion and is witnessed only in primary and secondary amines. The —CN stretching vibration of aliphatic amines showed a weak characteristic peak in the region of 1250–1020 cm^{-1}. While in aromatic amines, peaks are usually strong shown in Table 1 (Richner and Puxty 2012, Ismail et al., 2015).

Carboxylic acids showed a strong and wide peak for —OH stretch. Stretching peak of —OH seems to be wide at the frequency of about 3000 cm^{-1}. This peak appears in the same region as of —CH stretching bands of both alkyl and aromatic groups. Thus, carboxylic acid group here showed messy absorption pattern at 3300–2500 cm^{-1}, along with the broad —OH peak superimposed on the sharp —CH stretching peaks. All carbonyl compounds absorbed the frequencies in the region 1760–1665 cm^{-1} owing to the stretching vibration of the —C═O bond (Kamble and Gaikwad 2016).

Table 1 Comparative analysis of Monomer and Dimers vibrational modes.

Sr. no	Vibrational mode of Monomers	Frequency Range (cm^{-1})	Vibrational mode of Dimers	Frequency Range (cm^{-1})
1	—NH stretch	3400–3250	—C═O Stretch (Amide I)	1600–1800
2	—NH bend	1650–1580	—NH bend (Amide II)	1470–1570
3	—CN stretch (aromatic amines)	1335–1250	—CN coupled —NH in-plane bend (Amide III)	1250–1350
4	—CN stretch (aliphatic amines)	1250–1020	—NH Stretch (Amide A)	3300–3500
5	—NH wag	910–665	(Amide B)	3100–2500
6	—OH stretch	3300–2500	–	–
7	—C═O stretch	1760–1690	–	–

Irrespective of the amino acid monomers, the amide functional group of dimers combine the functionalities of both amines and ketones, therefore amides showed a very strong and broad peak of —NH stretch in the range of 3100–3500 cm^{-1}. At the same time, the stake-shaped peak at around 1710 cm^{-1} exhibits the presence of the —C═O stretch.

Characteristic peaks found in the spectra of dimers occur due to the amide bonds that connect the amino acids together, hence named Amide I and Amide II (Table 1). Peak of Amide I appeared due to the stretching vibrations of —C═O bond of the amide, while Amide II was found primarily due to the bending vibrations of —NH bond (Barth 2007, Júnior et al., 2015). Amide A corresponds to —NH stretching vibration, while the peak of Amide I corresponds to —C═O stretching character more intense than Amide II (Pérez-Mellor and Zehnacker, 2017).

The presence of peaks at 3100–3500 cm^{-1} relates to the amide group (Ji et al., 2020). Wide peaks in this range were observed in the spectrum of Glycine dimer and attributes to stretching of —NH group (Barth 2007, Júnior et al., 2015). Peaks at 3100–2600 cm^{-1} were observed due to vibrational symmetric and asymmetric stretching of —NH and —CH_2 groups. All these peaks correspond to the Amide B region (Başkan et al., 2015). The absorption peaks at 1700–1600 cm^{-1} identify amide —C═O group (Kristoffersen et al., 2020).

Amide I vibrational mode (1600–1690 cm^{-1}) appeared due to the combination of multiple —C═O stretch, —CN stretch and C—CN deformation. While in Amide II vibrational frequency (1480–1575 cm^{-1}) represents the resultant of —NH in-plane bend along with a —CN and C—C stretch. Other strong absorption peaks shown in Fig. 1 corresponds to different vibrational modes of —CN, —NH, C—C and —C═O group and confirm the formation of Glycine dimer (Pokorna et al., 2019).

Identical to the Glycine dimer, the rest of the amino acids studied in this paper give almost similar trend of characteristic peaks (Figs. 2–4) hence, confirms the successful formation of dimeric amino acid.

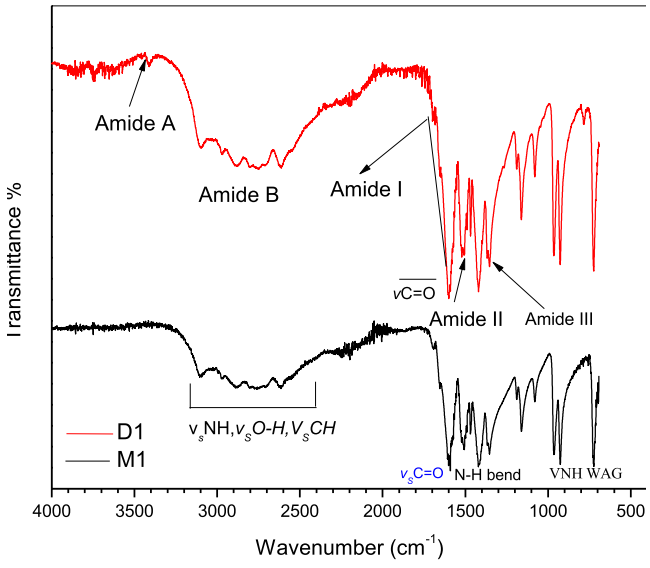

Fig. 1 FTIR spectra of glycine monomer(M1) and dimer (D1).

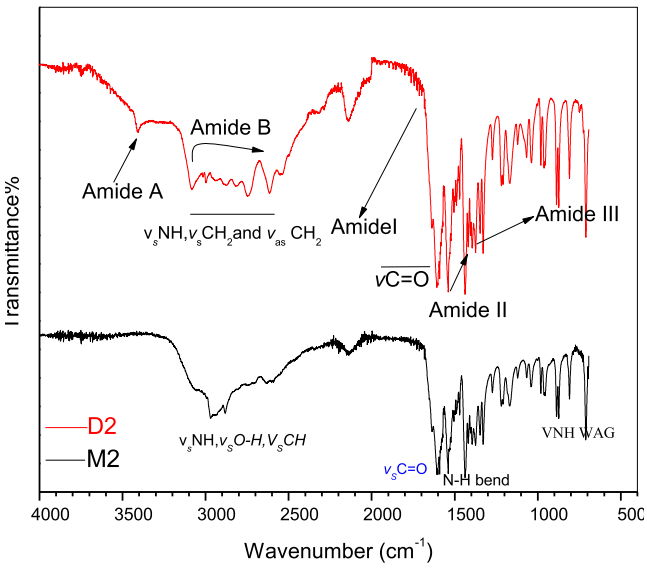

Fig. 2 FTIR spectra of leucine monomer (M2) and dimer (D2).

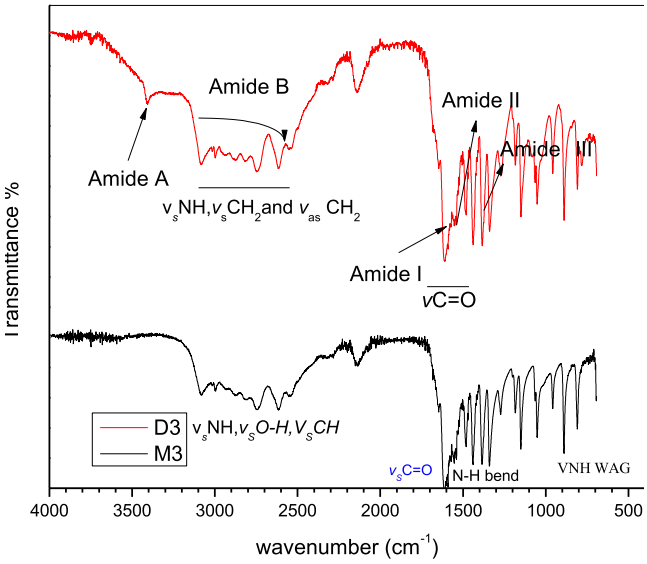

Fig. 3 FTIR spectra of alanine monomer (M3) and dimer (D3).

3.1.2. FTIR analysis of prodrugs

Co-crystals are direct product of self-assembly of an active pharmaceutical component and a co-former (Moisescu-Goia et al., 2017). Hence, to examine functional groups vibrational modes variations, FTIR was performed. In comparing to the chemical shift values for —NH and —C═O vibrations for 5-Fu, co-formers and co-crystals were attributed to the engagement of these groups in hydrogen bonding (Table 2). In spectra of 5-Fu (Fig. 5) wide peak at 3146 cm^{-1} could be assigned to —NH group relatively strong absorption band with high intensity at 1671 cm^{-1} is correspond to —C═O modes (Nadzri et al., 2016).

3.1.2.1. 5-Fu-GLY-D. Amino group in 5-Fu, appeared at higher frequency, i.e., 3146 cm^{-1}, after co-crystal development and this hypochromic shift (blue shift) specifies that intrinsic

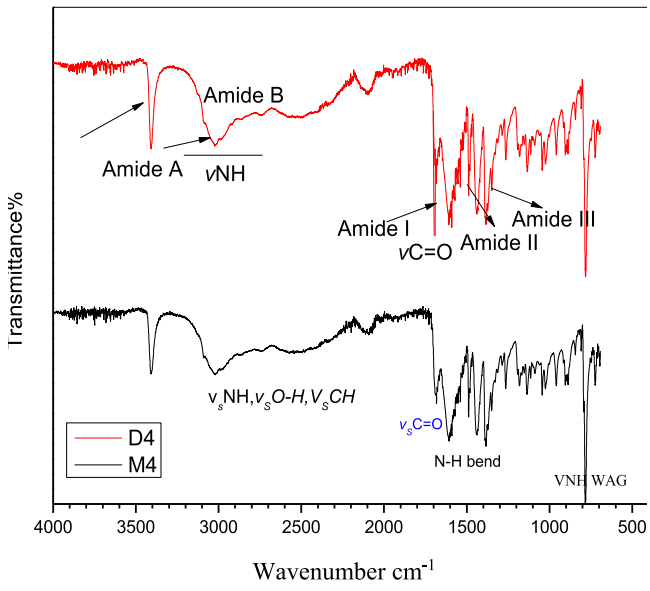

Fig. 4 FTIR spectra of Tryptophane monomer (M4) and dimer (D4).

Table 2 Absorption peaks comparison of groups liable for supramolecular interactions.

Sr no	Sample ID	v (C═O) cm^{-1}	v (N─H) str cm^{-1}
1	5-Fu	1671	3146
2	G.D	1669	3415
3	5Fu-G.D	1677	3486
4	A.D	1648	3408
5	5Fu-A.D	1680	3430
6	L.D	1641	3415
7	5Fu-L.D	1683	3459
8	T.D	1680	3415
9	5Fu-T.D	1689	3444

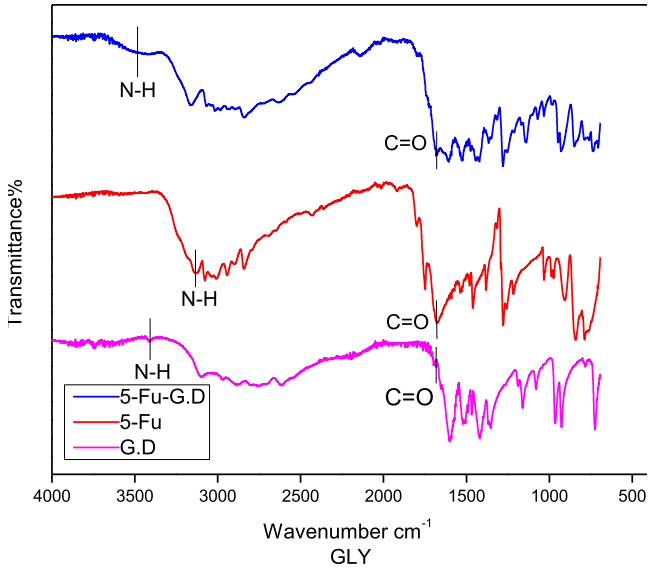

Fig. 5 FTIR spectra of Glycine dimer (G.D), 5-Fu and 5-Fu-G.D.

hydrogen bonding in 5-Fu is disconnected and new H-bonds are developed. Low intensity small peak arose at 3485 cm^{-1} succeeding the blue shift identified on the same trend in literature (Nadzri et al., 2016; Gautam et al., 2019). In fact, for 5-Fu-GLY-D solid form (Fig. 5), a similar blue shift was also noticed at 1677 cm^{-1} and the peak at the frequency of 1671 cm^{-1} was assigned to ─C═O stretching vibrations again accounts for hydrogen bonding interactions (Fig. 6). Co-crystals with interruption in the hydrogen bonding might improve the efficient aqueous solubility of a new solid form (Connelly et al., 2015).

3.1.2.2. 5-Fu-ALA-D. The ─NH peak for 5-Fu-ALA-D co-crystal (Fig. 7), was examined at 3430 cm^{-1} that manifests hypochromic shift as above case (Nadzri et al., 2016, Jubeen et al., 2019). Carbonyl groups were detected at 1680 cm^{-1} following the same regular hypochromic shift found as in 5-Fu-GLY-D. All the carbonyl groups and amide hydrogen were found to involve in bonding interaction as proposed in Fig. 8.

3.1.2.3. 5-Fu-LEU-D. 5-Fu-LEU-D co-crystal spectrum has shown a similar peaks trend found in the case of Leucine at 3459 cm^{-1} (Fig. 9). This similar trend validates hypochromic/blue shift as above case (Nadzri et al., 2016, Gautam et al., 2019). The regular hypochromic shift in the same compound was validated due to the observance of the peak at the frequency of 1683 cm^{-1}. This peak associated with the carbonyl functional group was found to involve in the bonding interactions as shown in Fig. 10.

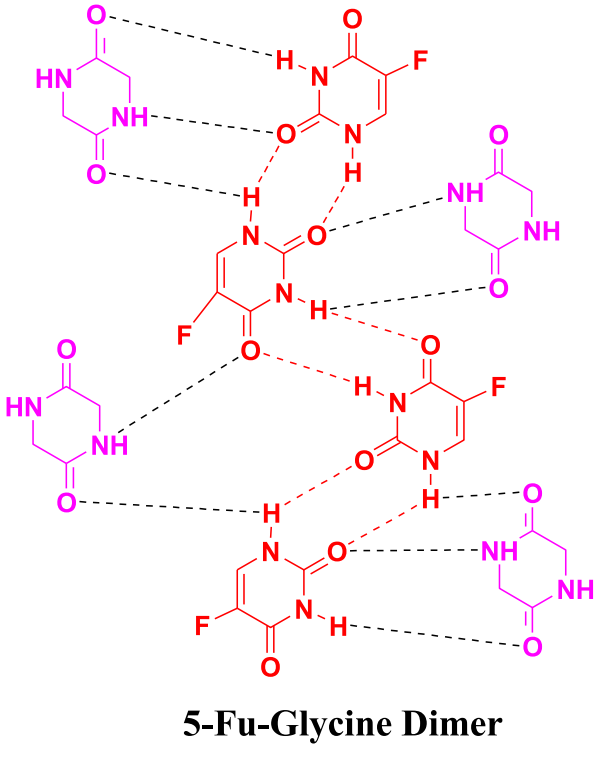

Fig. 6 Proposed interactions in 5-Fu-G.D (5-Fu-Glycine Dimer) co-crystals.

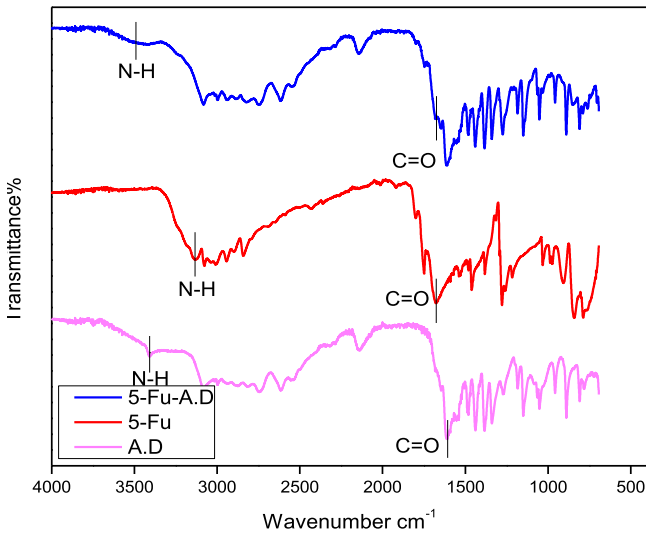

Fig. 7 FTIR spectra of Alanine dimer (A.D), 5-Fu and 5-Fu-A.D.

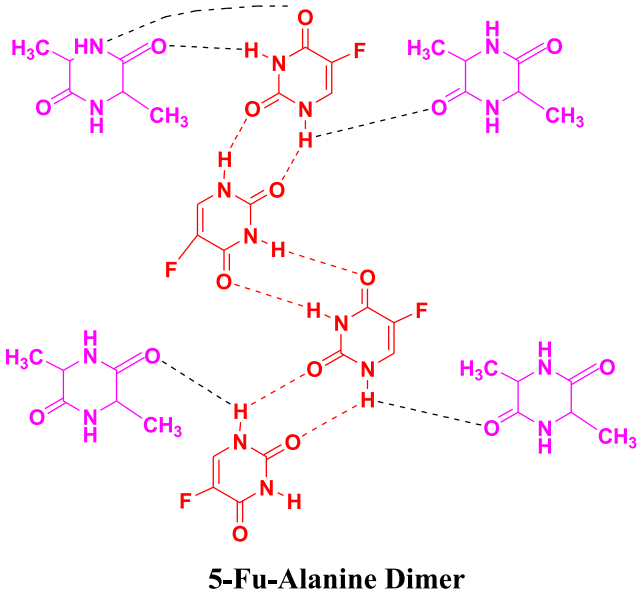

Fig. 8 Proposed interactions in 5-Fu-A.D (5-Fu-Alanine Dimer) co-crystals.

3.1.2.4. 5-Fu-TRY-D. The —NH frequency peak for 5-Fu-TRY-D co-crystal was seen at 3444 cm^{-1} (Fig. 11), exhibits the same blue shift (Nadzri et al., 2016; Jubeen et al., 2020). Carbonyl groups were seen at 1689 cm^{-1} that indicated the same regular hypochromic shift and bonding interactions (Fig. 12). Conclusively, in all the newly developed co-crystals, noteworthy changes in absorption frequencies of peaks with similar trends were observed. Results are in the favor of an efficient establishment of new interactions.

3.2. Structural analysis

Co-crystals were further confirmed via powdered XRD. Peaks shift of 5-Fu are noteworthy in all co-crystal forms. These

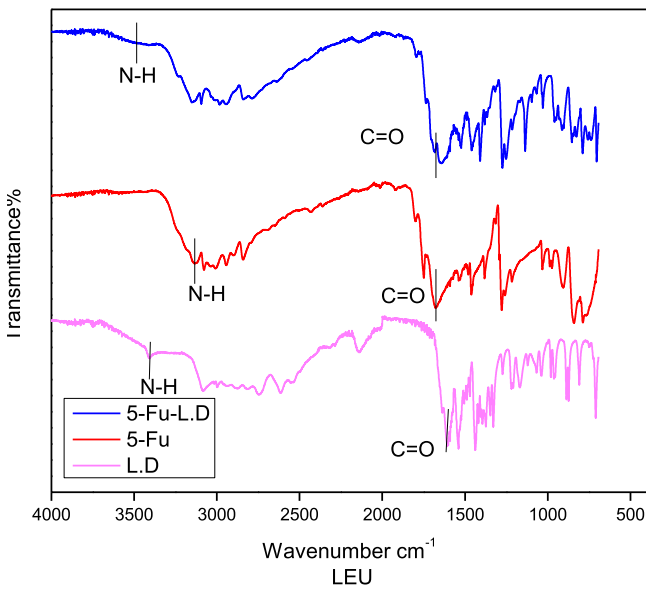

Fig. 9 FTIR spectra of Leucine dimer (L.D), 5-Fu and 5-Fu-L.D.

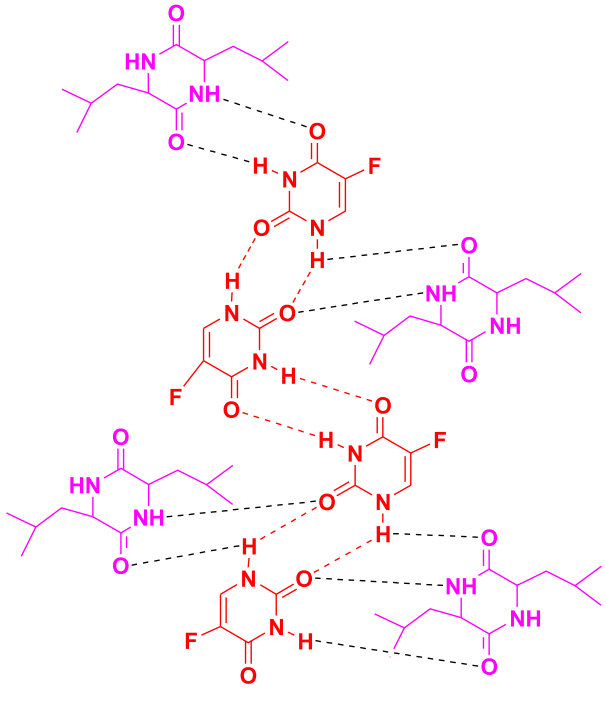

Fig. 10 Proposed interactions in 5-Fu-L.D (5-Fu-Leucine Dimer) co-crystals.

shifts indicate the structural variation of 5-Fu because of the change in molecular contacts with distinct co-formers (Moisescu-Goia et al., 2017; Jubeen et al., 2020).

In the spectrum (Fig. 13), sharp peak of 5-Fu at $2\theta = 28.48$ is equal to the range stated in the literature (Moisescu-Goia et al., 2017). This distinguishing value of 5-Fu moved in co-crystals graphs.

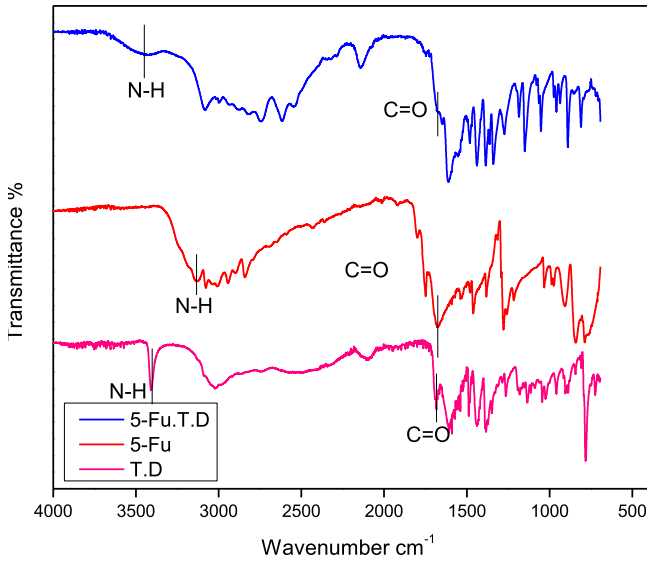

Fig. 11 FTIR spectra of Tryptophane dimer (T.D), 5-Fu and 5-Fu-T.D.

Sharp peak was seen at 2θ = 29.98 for 5-Fu-G.D. Also, FWHM values are differed than the values noted for 5-Fu (Table 3). Smaller FWHM value indicates the significantly larger size of co-crystals than API, demonstrating the existence of both constituents in the synthesized co-crystals.

Another evident 5-Fu-A.D peak was noted at 2θ = 20.96. This peak strength and size is greater than API confirming the improved crystal nature of co-crystal. Same trend regarding intensity of the peaks is observed for newly synthesized 5-Fu-L.D and 5-Fu-T.D co-crystals. Variation in 2θ values, intensities, FWHM ranges and crystalline sizes are assembled in (Table 3).

Few new peaks are detected in the co-crystals graphs and many peaks which seen in the 5-Fu graph are lost in the co-crystal's graphs. The substantial variations in the frequency ranges and new peaks indicate alterations in 5-Fu system also manifest the modifications in supra-molecular interfaces due to attachment of different co-formers. All co-crystals and API size is shown in Table 3 (Li et al., 2014a). Conclusively, new solid forms crystal size indicates the effective development of sturdy hydrogen bonding in all co-crystals. This interpretation manifests the successful formation of supramolecular synthons having both co-former and API components.

3.3. In vitro anticancer activity

To evaluate the inhibition rate, we carried out 3-(4,5-dimethyl-2-thiazolyl)-2,5- diphenyl-2-H-tetrazolium bromide (MTT) assay on two tumor cell lines. Reference/Standard drug used in this study was Doxorubicin and anticancer activity was compared with newly synthesized co-crystals of 5-Fu against MCF7 breast and SW480 colon cancer cell lines. Tables 4 and 5 includes the percentage inhibition rate at nine doses concentrations against two tumor cell lines. For the most efficient anticancer agent assessment, inhibition rates are presented in Fig. 14 and Fig. 15. Examined values showed that actinomycetes concentrations and percentage of inhibition are related to each other as the actinomycetes concentration is greater, the percentage of inhibition is likewise higher. At 200 ug/mL maximum growth inhibition percentage is seen for 5-Fu and new solid forms. This trend line is fairly logical, as microorganism extract concentration is increased, reactive sites for the newly synthesized drugs to implement anticancer activity is also improved and consequently the inhibition rate is also increased (Fang et al., 2015).

It is apparent from the assessment of all the 5-Fu co-crystals, that 5-Fu-L.D and 5-Fu-T.D co-crystals showed max-

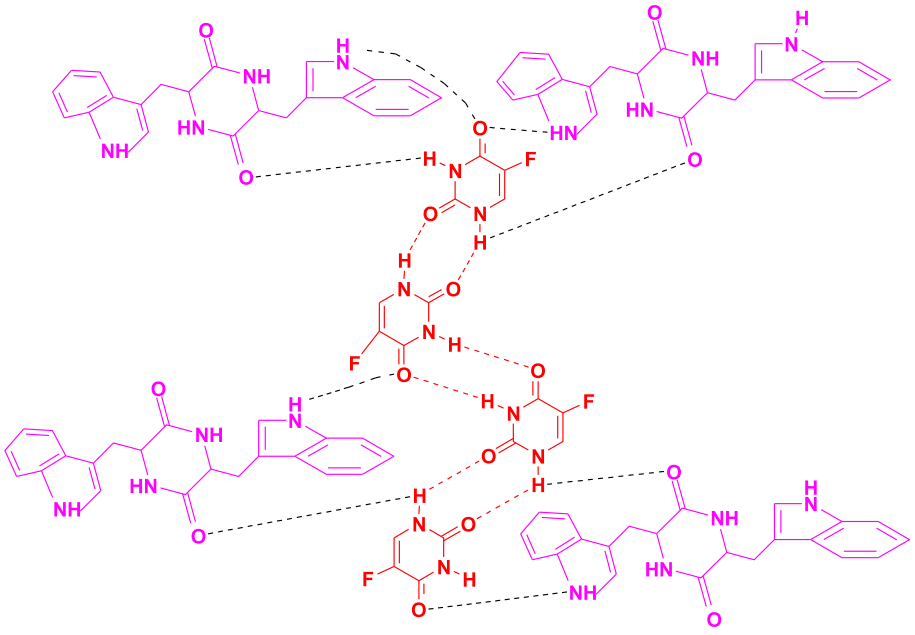

Fig. 12 Proposed interactions in 5-FU-T.D (5-Fu-Tryptophane Dimer) co-crystals.

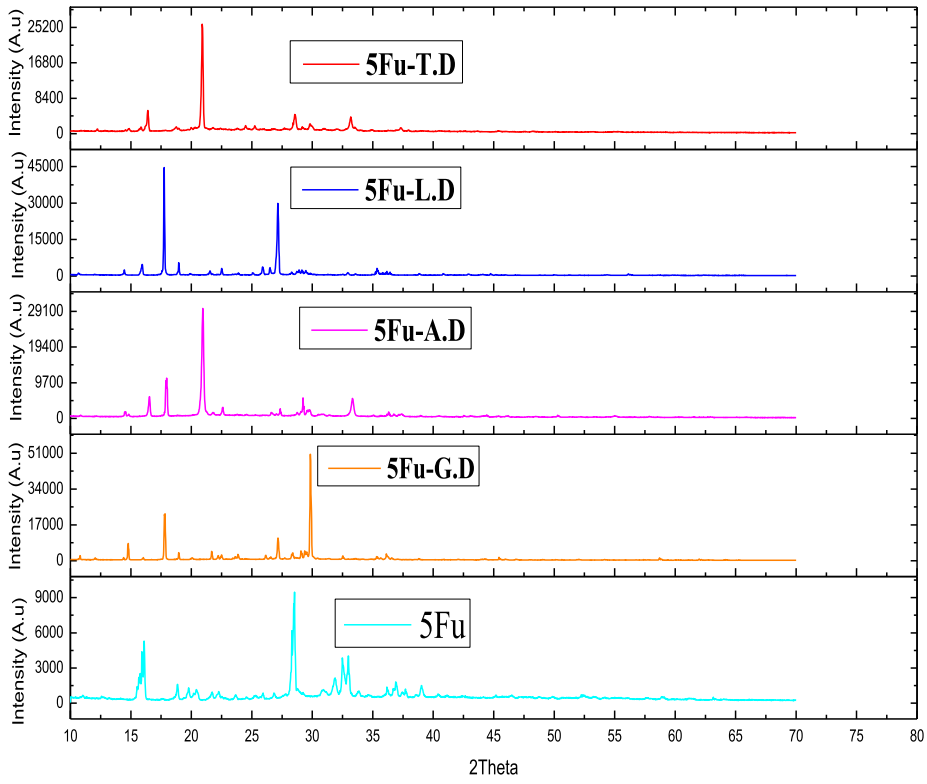

Fig. 13 XRD pattens of API and Co-formers synthesized by solution method.

Table 3 Comparison between the most prominent peaks of 5-Fu alone and its co-crystal.

Sr. no	Sample ID	2 θ (°)	Intensity	FWHM	Crystalline size (nm)
1	5-Fu	28.48	9380	0.29	282.51
2	5Fu-G.D	29.98	50,311	0.12	685.07
3	5Fu-A.D	20.96	29,841	0.20	403.79
4	5Fu-L.D	18.06	43,838	0.09	893.42
5	5Fu-T.D	21.14	26,110	0.16	504.89

Table 4 Inhibition rate (%) against SW 480 (Colon cancer cell line) using different concentration.

Conc (μM)	5-Fu-G.D	5-Fu-A.D	5-Fu-L.D	5-Fu-T.D	5-Fu
200	81	72	100	99	79
100	43	31	100	97	64
50	36	22	100	88	53
25	29	17	93	79	39
12.5	20	12	81	60	19
6.25	16	0	75	47	3
3.13	11	0	59	39	0
1.56	9	0	48	27	0
0.78	7	0	37	20	0

imum tumor constraining agents at all nine concentrations against SW 480colon cancer cell line. At 200 dose concentration, the efficacy of 5-Fu-L.D is 100 % and for 5-Fu-T.D is 99 %, maximum amongst all the developed new solids forms. The reason this trend may be the antitumor potency of Leucine and Tryptophane monomers and dimers itself. Leucine

Table 5 Inhibition rate (%) against using MCF 7 (Breast cancer) cell line different concentration.

Conc (μM)	5-Fu-G.D	5-Fu-A.D	5-Fu-L.D	5-Fu.T.D	5-Fu
200	79	100	84	100	84
100	36	100	67	100	40
50	29	100	48	100	27
25	24	96	19	94	19
12.5	22	83	0	88	13
6.25	7	72	0	80	0
3.12	0	67	0	70	0
1.56	0	58	0	62	0
0.78	0	49	0	59	0

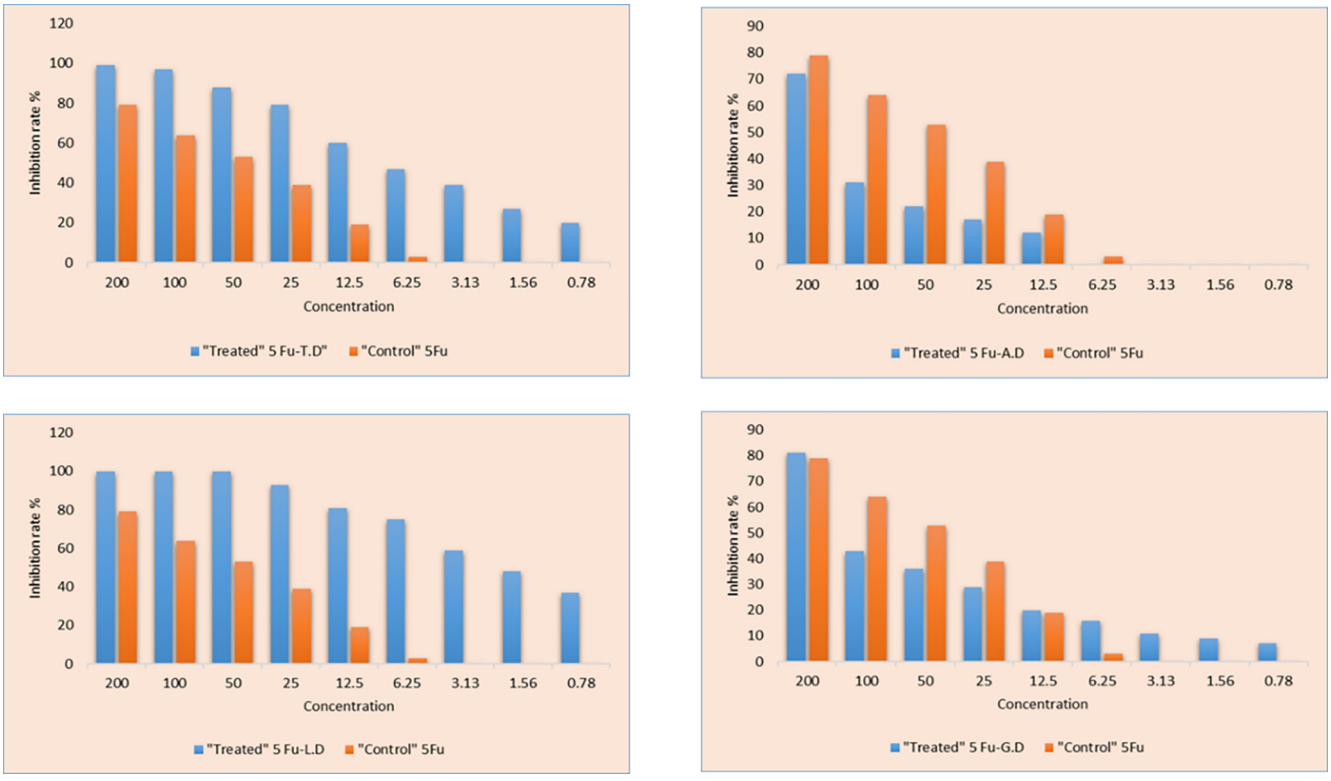

Fig 14 The MTT assay showing inhibition rate (%) of synthesized prodrugs against SW 480 (Colonic cancer cell line) at different concentration.

dimmer/zipper derivatives has been widely studied and used as potent antitumor mediators (Li et al., 2014b; Prabha et al., 2020; Zhou et al., 2021).

While the other new solid forms have varied trend. Though, at 200 μg/mL, 5-Fu-G.D has more inhibition rate 81 % than 5-Fu (79 %). Inhibition rate (%) of co-crystals against MCF 7 breast cancer cell line have also mixed trends. Best results of co-crystals concerning MTT test might be accredited to the willingly API release to the target sight and 5-Fu improved efficacy is because of co-formers pharmaceutical efficacy. Slightly different inhibiting percentages of 5-Fu and co-crystals may be due to distinct structural feature of conformers and varied interactions.

Recently in 2020 co-crystals of 5-Fluorouracil with organic acids have been reported by Jubeen and her co-researchers. In this study 5-Fu-Cinnamic acid was proved as highly effective anticancer mediator with 67.29 % inhibition rate at highest concentration (100 μg/mL) (Jubeen et al., 2020).

Similarly, Co-crystals of 5-Fu with pharmacologically active co-formers e.g., Urea, Thiourea, Acetanilide and Aspirin were reported by (Jubeen et al., 2019). Tumor growth inhibition percentage was also detected by the researchers in this study via *in vitro* MTT assay and results revealed that 5-Fu–Acetanilide and 5-Fu-(Thiourea) have highest anticancer potential, i.e., 80.51 % among others (Jubeen et al., 2019).

With comparison to these previously developed co-crystals, newly developed co-crystals with Leucine and Tryptophane dimer showed more efficacy toward SW 480 Colon Cancer cell line at all concentration than 5-Fu alone (Table 4). Against MCF 7 (Breast Cancer) cell line, 5-Fu co-crystals with Alanine

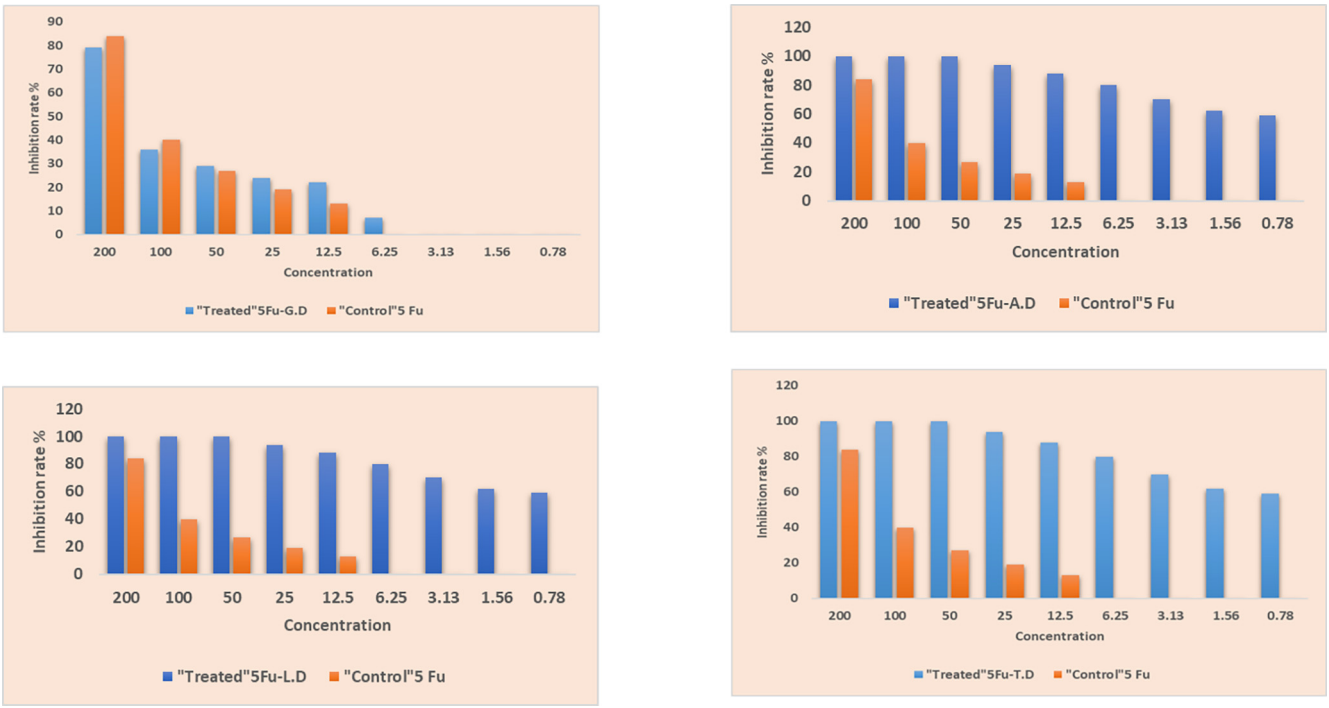

Fig 15 The MTT assay showing inhibition rate (%) of synthesized prodrugs against MCF 7 (Breast cancer) cell line at different concentration.

and Tryptophane dimer showed more efficacy than 5-Fu alone (Table 5).

3.4. Ligand protein interaction

Structural examination was carried out of the connections among the proteins and 5-Fu using the MOE (Molecular Operating Environment) software. The details of the interactions are explained ahead. The percentage threshold of interaction was set to 30 %. Therefore, all the interacting residues shows greater than 30 % interactions.

3.4.1. Thymidylate synthase - PDB ID: 1HVY

3.4.1.1. Alanine and 5-Fluorouracil. The hydroxyl of Tyr135 shares H-bond with carbonyl of 5′-Fluorouracil. Amino group of Cys195 makes H-bond by carbonyl of 5′-Fluorouracil. Additionally, sulfur (S) shares hydrogen bonding with carbonyl and amino group of 5′-Fluorouracil as well as with carbonyl group of alanine. Here, it is elucidated that there is no direct interaction between alanine and 5′-Fluorouracil, but indirect interaction with the help of sulfur atom is present. It can be said that this sulfur is playing a linker role and enabled a unique system of interactions within the protein–ligand complex. Moreover, the carbonyl group of alanine shares H-bonding with amino of Asp218and carbon atom of Gly217 (Fig. 16a).

3.4.1.2. Glycine and 5-Fluorouracil. 5′-fluorouracil interacts with sulfur atom of Cys195 and carbonyl group of glycine with its amino group. There is a direction interaction between glycine and 5′-Fluorouracil. The H-bond interactions around carbonyl group of glycine are very rich. Carbonyl group interaction with amino groups of Arg50 and sulfur atom of Cys195 is present. This indicates stability and strength of the protein–ligand complex. Moreover, the other carbonyl group of glycine develops H-bonding with amino of Lys47 (Fig. 16b).

3.4.1.3. Leucine and 5-Fluorouracil. A number of interactions of leucine; its carbonyl group, amino group and carbon atom forms H-bond with amino group of Asn226, carbonyl group of Ile108 and sulfur atom of Met311 respectively. 5′-Fluorouracil has H-bond between its carbonyl group and Arg50′s amino group. Moreover, amino group of Ala312 makes H-bond with carbonyl group of 5′-Fluorouracil. Although there is absence of direct interaction between leucine and 5′-Fluorouracil, the two structures are well bonded inside the protein–ligand complex (Fig. 16c).

3.4.1.4. Tryptophan and 5-Fluorouracil. 5′-Fluorouracil has a strong network of interactions around it. The two-carbonyl group of 5′-Fluorouracil have H-bond interactions, each with atoms of unique neighboring residues. First carbonyl group of 5′-Fluorouracil forms H-bond with carbon atom of tryptophan residue while the second carbonyl group has H-bonds with carbon atom and hydroxyl group of Tyr135. There is direct interaction established between 5′-Fluorouracil and tryptophan. H-bond interactions is present between amino group of 5′-Fluorouracil and carbonyl group of Asn226.The other amino group of 5′-Fluorouracil shares H-bond with Sulfur atom of Cys195. The sulfur atom of Cys195 has H-bond

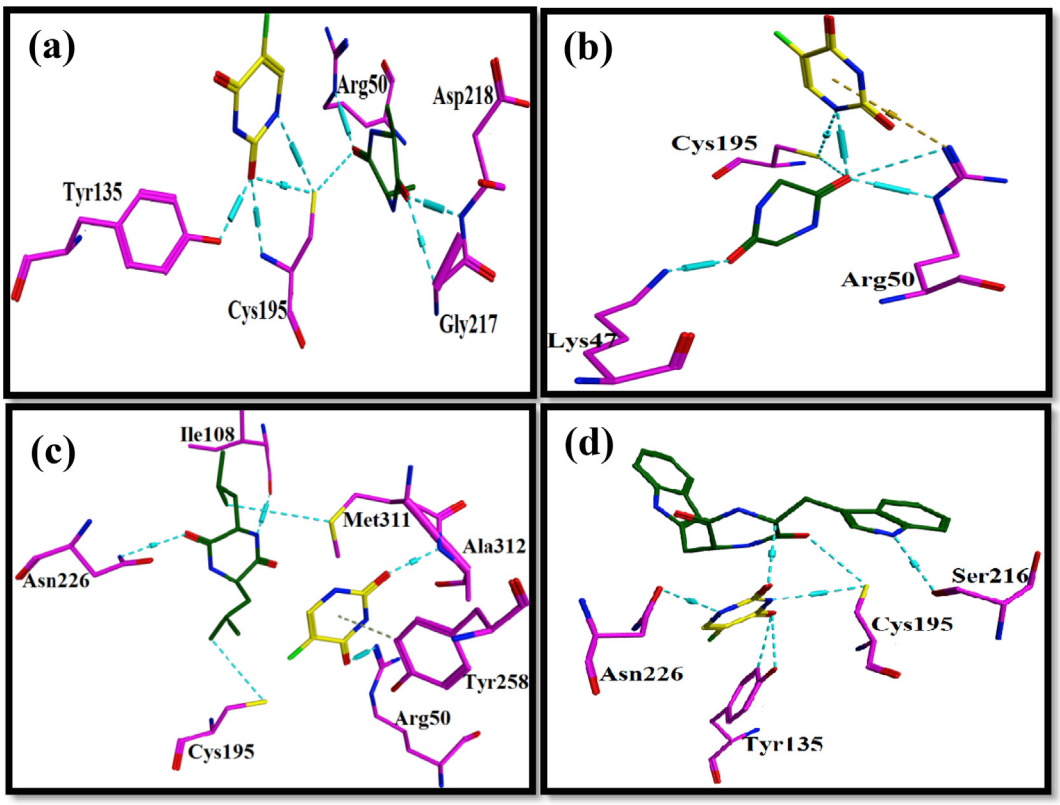

Fig. 16 Amino acids derivatives are represented in green, 5-Fluorouracil in yellow inside the binding pocket of Thymidylate synthase where cyan dotted lines represent the H-bonds. (a) Represents the interaction of alanine with 5-Fluorouracil with 1HVY, (b) shows the interaction profile of Glycine and 5-Fluorouracil with 1HVY, (c) shows the interaction of Leucine and 5-*F*luorouracil 1HVY (d) represents the interaction profiles of the Tryptophan and 5-Fluorouracil with 1HVY structure of the Thymidylate synthase.

with carbonyl of tryptophan. Carbonyl of Ser216 has H-bond interactions with tryptophan (Fig. 16d).

3.4.2. AKT3 Protein Kinase - PDB ID: 2X18

3.4.2.1. Alanine and 5-Fluorouracil. The amino group of Alanine residue forms H-bond with carbonyl group of 5′-Fluorouracil. Alanine's carbonyl group shares H-bond with amino group of Arg85, which further interacts with carbonyl group of 5′-Fluorouracil. It can be seen that there is direct and indirect interaction between alanine and 5′-Fluorouracil. Carbonyl group of 5′-Fluorouracil has H-bond with amino group of Asn52. Amino group of 5′-Fluorouracil interacts with carbonyl group of Glu17 though H-bond (Fig. 17a).

3.4.2.2. Glycine and 5-Fluorouracil. Glycine's carbonyl forms H-bond between two amino groups of Arg85. Carbonyl group of 5′-Fluorouracil has H-bond with amino of Asn53 (Fig. 17b).

3.4.2.3. Leucine and 5-Fluorouracil. The carbonyl group of leucine residue forms H-bonding by Arg85 amine group. Leucine amine group shares H-bond with Asn53 carbonyl group. The amino group 5′-Fluorouracil shares H-bond with carbonyl group of Arg75. 5′-Fluorouracil carbonyl group forms two H-bond with Cys76. One with the carbon atom and other with the sulfur atom. Carbonyl of Gln78 and amine of 5′-Fluorouracil interact through H-bond. The interaction of 5′-Fluorouracil with the neighboring protein's residues indicates its stable conformation inside the protein–ligand complex (Fig. 17c).

3.4.2.4. Tryptophan and 5-Fluorouracil. Both carbonyl groups of tryptophan forms H-bond with amino groups of Asp90 and Trp11. Additionally, amino group of tryptophan shares H-bond with carbonyl group of Gln13 (Fig. 17d).

3.4.3. CMYC - PDB ID: 6G6K

3.4.3.1. Alanine and 5-Fluorouracil. Alanine has H-bond with carbonyl group of Glu916. Carbonyl group of alanine shares H-bonding with Arg919 amino group. Lys918 amino group interacts by the carbonyl group of 5-fluorouracil. There is no direct interaction between alanine and 5-Fluorouracil, but Arg919 and Lys918 serve as a bridge between the two structures. Amino group of 5-Fluorouracil develops H-bonding with Ala937 carbonyl group. Other 5-Fluorouracil amino group makes H-bond with carbonyl of Glu935 (Fig. 18a).

3.4.3.2. Glycine and 5-Fluorouracil. The two carbonyl groups of glycine form H-bonds with amino group of Arg919 and

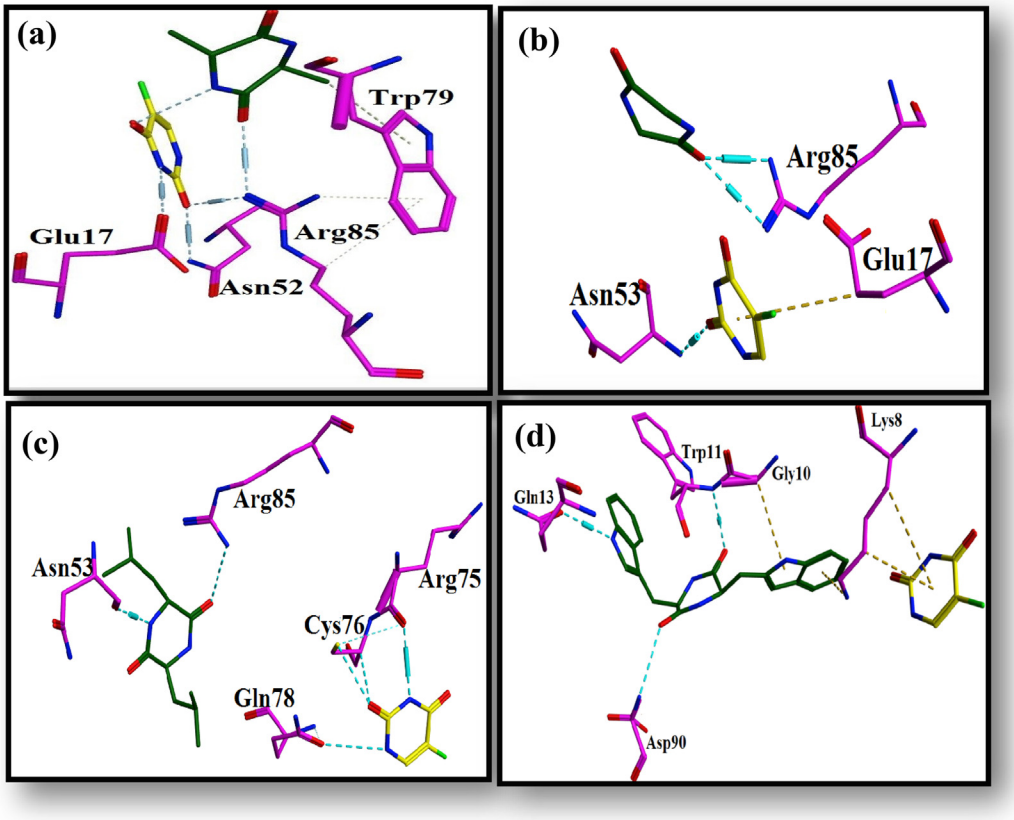

Fig. 17 Ligand protein interaction profiles of 5-Fluorouracil in yellow and (a) Alanine, (b) Glycine, (c) Leucine and (d) Tryptophane in green inside the binding pocket of AKT3 Protein Kinase where cyan dotted lines represent the H-bonds.

oxygen atom of Ser920. 5′-Fluorouracil carbonyl group form H-bond with amino group and carbon atom of Arg919. Moreover, amino group of 5′-Fluorouracil has H-bond with carbonyl group of Glu935. H-bond interactions around Arg919 facilitate 5-Fluorouracil and glycine (Fig. 18b).

3.4.3.3. Leucine and 5-Fluorouracil. The two carbonyl groups of leucine residue forms Hydrogen bond with carbonyl of Ser920 and amino of Arg919. Amino group of leucine has H-bond with Glu916 carbonyl group. 5-Fluorouracil carbonyl groups have H-bonds with amino groups of Lys939 and Arg914. Additionally, amino group of 5-Fluorouracil shares H-bond with Asn915 carbonyl group. 5-Fluorouracil and leucine are very far from each other yet the strong interactions of these structures within the binding pocket of protein allows stability of overall complex (Fig. 18c).

3.4.3.4. Tryptophan and 5-Fluorouracil. Tryptophan amino group develops H-bond with amino group of Arg919. Second amino group of Arg919 shares H-bond with carbonyl group of 5-Fluorouracil. Tryptophan and 5-Fluorouracil do not interact directly but they are held firmly in binding pocket of protein through Arg919. Furthermore, amino groups of tryptophan are seen to have H-bonds with carbonyl group of Glu935 and carbonyl group of Phe922. 5-Fluorouracil can be seen sharing hydrogen bonding with carbonyl group of Glu916 (Fig. 18d).

3.5. Box plots

3.5.1. Thymidylate synthase – 1HVY

The range of the gold fitness score for 5-Fluorouracil docked poses within the binding cavity of Thymidylate synthase for the amino acid residues (Fig. 19) are as follows:

Alanine: 20.4083–17.2907, Glycine: 35.9310–33.0785, Leucine: 31.5361–14.2384, Tryptophan: 26.9961–24.8847.

3.5.2. Protein kinase – 2X18

The range of the gold fitness score for 5-Fluorouracil docked poses within the binding cavity of Protein kinase for the amino acid residues (Fig. 20) are as follows:

Alanine: 22.9516–15.3526, Glycine: 21.0056–17.3257, Leucine: 25.2033–12.3629, Tryptophan: 27.8153–16.1950.

3.5.3. CMYC – 6G6K

The range of the gold fitness score for 5-Fluorouracil docked poses within the binding cavity of CMYC for the amino acid residues (Fig. 21) are as follows:

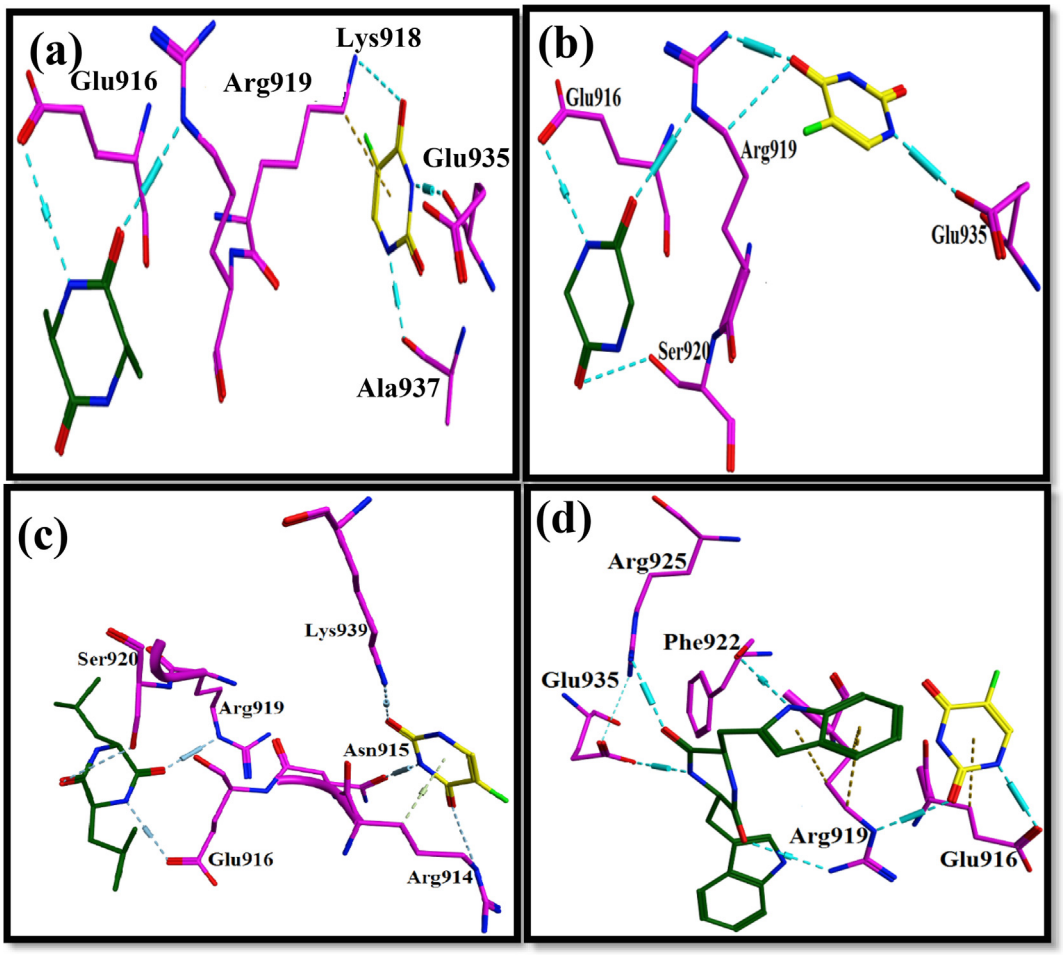

Fig. 18 Ligand protein interaction profiles of 5-Fluorouracil in yellow and (a) Alanine, (b) Glycine, (c) Leucine and (d) Tryptophane in green inside the binding pocket of C-MYC Protein Kinase where cyan dotted lines represent the H-bonds.

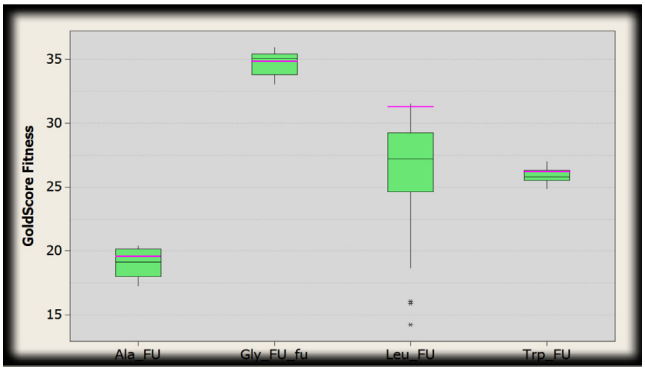

Fig. 19 Box plot indicating the distribution of Gold fitness score. The green boxes represent docked conformations of conjugated structure of thymidylate synthase and amino acid residues (alanine, glycine, leucine and tryptophan) with 5-Fluorouracil. Pink line shows the GoldScore selected where intermediate interactions were comparatively better.

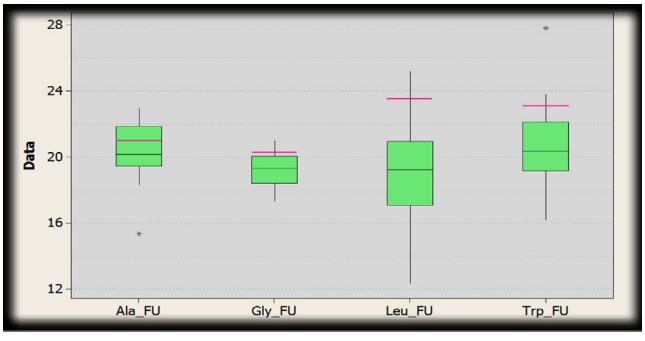

Fig. 20 Box plot indicating the distribution of Gold fitness score. The green boxes represent docked conformations of conjugated structure of Protein Kinase and amino acid residues (alanine, glycine, leucine and tryptophan) with 5-Fluorouracil. Pink line shows the GoldScore selected where intermediate interactions were comparatively better.

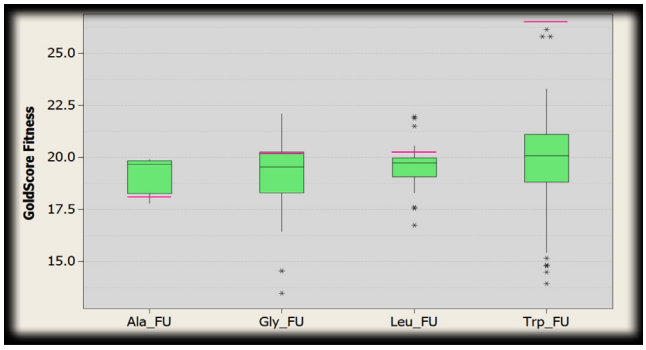

Fig. 21 Box plot indicating the distribution of Gold fitness score. The green boxes represent docked conformations of conjugated structure of CMYC and amino acid residues (alanine, glycine, leucine and tryptophan) with 5-Fluorouracil. Pink line shows the GoldScore selected where intermediate interactions were comparatively better.

Alanine: 19.9013–17.7785, Glycine: 22.0950–13.4770, Leucine: 21.9627–16.7279, Tryptophan: 26.1427–13.9184.

4. Conclusion

Four Cyclic dimers of amino acids (Glycine, Leucine, Alanine and Tryptophane) were prepared by thermal condensation and then utilizing these as co-formers, co-crystals of 5-Fu were synthesized via solution procedure with no byproducts. FTIR results indicated that main amine and carbonyl peaks were distinctly moved in all co-crystal's spectra. These shifts are reminiscent of variations in the 5-Fu intermolecular interactions. Likewise, in PXRD spectra many different peaks were noted showing the advancement of entirely different parts after co-crystallization. Anticancer efficacy was assessed via MTT assay against SW 480 Colon and MCF 7 Breast cancer cell lines at nine different strengths of integrated co-crystals, which turn out to be efficient than 5-Fu (API) alone indicating effective fabrication plan with improved anticancer potential. Computational study was applied using GOLD software against different target proteins. To sum up, this work confirmed the formation of new 5-Fu prodrugs by following easy synthesis technique, conditions and showed highest anticancer potential of newly developed co-crystals than the previously reported 5-Fu co-crystals and 5-Fu alone. These 5-Fu co-crystals can be used in the anticancer study and further assessment for *in vivo* safety trials. Additionally, others anti-tumor efficient dimers co-formers can be also be studied in future work.

Funding

This research was funded by Princess Nourah bint Abdulrahman University Researchers Supporting Project number (PNURSP2022R95), Princess Nourah bint Abdulrahman University, Riyadh, Saudi Arabia.

Declaration of Competing Interest

The authors declare that they have no known competing financial interests or personal relationships that could have appeared to influence the work reported in this paper.

Acknowledgements

The authors express their gratitude to Princess Nourah bint Abdulrahman University Researchers Supporting Project number (PNURSP2022R95), Princess Nourah bint Abdulrahman University, Riyadh, Saudi Arabia. The authors extend their appreciation to the Deanship of Scientific Research at King Khalid University, Saudi Arabia for funding this work through the Research Groups Program under grant number R.G.P.1:255/43.

References

Abdellatif, H., Abd El Rady, E., 2020. Synthesis of naphtho-quinoxaline-7, 12-dione, anthra-ptereidine-7, 12-dione and anthra-pyridine derivatives. Chem. Int. 6, 200–209.

Abdellatif, H., El Rady, E.A., 2020. Facile route for the synthesis and characterization of new naphtho [2, 3-f] quinoxaline-dione, trione and anthra-dione derivatives. Chem. Int. 6, 122–130.

Aftab, U., Sajid, I., 2017. Antitumor peptides from Streptomyces sp. SSA 13, isolated from Arabian Sea. Int. J. Pept. Res. Ther. 23, 199–211.

Al-Anazi, M., Khairuddean, M., Al-Najjar, B.O., et al, 2022. Synthesis, anticancer activity and docking studies of pyrazoline and pyrimidine derivatives as potential epidermal growth factor receptor (EGFR) inhibitors. Arab. J. Chem. 15, 103864.

Albratty, M., Alhazmi, H.A., 2022. Novel pyridine and pyrimidine derivatives as promising anticancer agents: A review. Arab. J. Chem. 15, 103846.

Amos-Tautua, B.M., Fakayode, O., Songca, S.P., et al, 2020. Synthesis, spectroscopic characterization and singlet oxygen generation of 5,10,15,20-tetrakis(3,5-dimethoxyphenyl) porphyrin as a potential photosensitizer for photodynamic therapy. Chem. Int. 5, 10–15.

Arango, D., Mariadason, J., Wilson, A., et al, 2003. c-Myc overexpression sensitises colon cancer cells to camptothecin-induced apoptosis. Br. J. Cancer 89, 1757–1765.

Barth, A., 2007. Infrared spectroscopy of proteins. Biochimica et Biophysica Acta (BBA)-Bioenergetics 1767, 1073–1101.

Başkan, M.H., Kartal, Z., Aydın, M., 2015. Electron paramagnetic resonance and FT-IR spectroscopic studies of glycine anhydride and betaine hydrochloride. Radiat. Eff. Defects Solids 170, 989–997.

Benaka Prasad, S.B., Anandakumar, C.S., Raghu, A.V., et al, 2018a. Synthesis, structural exploration and Hirshfeld surface analysis of a novel bioactive heterocycle: (4-(6-Fluorobenzo[d]isoxazol-3-yl) piperidin-1-yl)(morpholino)methanone. Chem. Data Collect. 15–16, 1–9.

Benaka Prasad, S.B., Naveen, S., Ananda Kumar, C.S., et al, 2018b. Synthesis, structural exploration, spectral and combinatorial analysis of racemic-3-isobutyl-5-phenyl-5-(pyridin-4-yl)imida-zolidine-2,4-dione: Comparison between experimental and DFT calculations. J. Mol. Struct. 1167, 215–226.

Buikhuisen, J.Y., Gomez Barila, P.M., Torang, A., et al, 2021. AKT3 expression in mesenchymal colorectal cancer cells drives growth and is associated with epithelial-mesenchymal transition. Cancers 13, 801.

Carrillo, E., Navarro, S.A., Ramírez, A., et al, 2015. 5-Fluorouracil derivatives: a patent review (2012–2014). Expert Opin. Ther. Pat. 25, 1131–1144.

Connelly, P.R., Snyder, P.W., Zhang, Y., et al, 2015. The potency–insolubility conundrum in pharmaceuticals: Mechanism and solution for hepatitis C protease inhibitors. Biophys. Chem. 196, 100–108.

Dai, X.-L., Li, S., Chen, J.-M., et al, 2016. Improving the membrane permeability of 5-fluorouracil via cocrystallization. Cryst. Growth Des. 16, 4430–4438.

Danenberg, P.V., Malli, H., Swenson, S., 1999. Thymidylate synthase inhibitors. Sem. Oncol.

de Oliveira, B.E., Amorim, O.H.J., Lima, L.L., et al, 2020. 5-Fluorouracil, innovative drug delivery systems to enhance bioavailability for topical use. J. Drug Delivery Sci. Technol. 102155.

Deeba, F., Abbas, N., Butt, M.T., et al, 2018. Synthesis, characterization and biological activities of 1, 3, 4-oxadiazole derivatives of nalidixic acid and their copper complexes. Chem. Int. 4, 206–215.
Delori, A., Eddleston, M.D., Jones, W., 2013. Cocrystals of 5-fluorouracil. CrystEngComm 15, 73–77.
Entezar-Almahdi, E., Mohammadi-Samani, S., Tayebi, L., et al, 2020. Recent advances in designing 5-fluorouracil delivery systems: a stepping stone in the safe treatment of colorectal cancer. Int. J. Nanomed. 15, 5445.
Fang, F.-Q., Guo, H.-S., Zhang, J., et al, 2015. Anti-cancer effects of 2-oxoquinoline derivatives on the HCT116 and LoVo human colon cancer cell lines. Mol. Med. Rep. 12, 8062–8070.
Ferlay, J., Colombet, M., Soerjomataram, I., et al, 2019. Estimating the global cancer incidence and mortality in 2018: GLOBOCAN sources and methods. Int. J. Cancer 144, 1941–1953.
Gautam, M.K., Besan, M., Pandit, D., et al, 2019. Cocrystal of 5-fluorouracil: characterization and evaluation of biopharmaceutical parameters. AAPS PharmSciTech. 20, 1–17.
Gu, J., Li, Z., Zhou, J., et al, 2019. Response prediction to oxaliplatin plus 5-fluorouracil chemotherapy in patients with colorectal cancer using a four-protein immunohistochemical model. Oncol. Lett. 18, 2091–2101.
Hinz, N., Jücker, M., 2019. Distinct functions of AKT isoforms in breast cancer: a comprehensive review. Cell Commun. Signal. 17, 1–29.
Hong, S., Cai, W., Huang, Z., et al, 2020. Ginsenoside Rg3 enhances the anticancer effect of 5-FU in colon cancer cells via the PI3K/Akt pathway. Oncol. Rep. 44, 1333–1342.
Ismail, H., Mirza, B., Haq, I.-U., et al, 2015. Synthesis, characterization, and pharmacological evaluation of selected aromatic amines. J. Chem. 2015.
Ji, Y., Yang, X., Ji, Z., et al, 2020. DFT-calculated IR spectrum amide I, II, and III band contributions of N-methylacetamide fine components. ACS Omega 5, 8572–8578.
Jubeen, F., Iqbal, S.Z., Shafiq, N., et al, 2018. Eco-friendly synthesis of pyrimidines and its derivatives: A review on broad spectrum bioactive moiety with huge therapeutic profile. Synth. Commun. 48, 601–625.
Jubeen, F., Liaqat, A., Sultan, M., et al, 2019. Green synthesis and biological evaluation of novel 5-fluorouracil derivatives as potent anticancer agents. Saudi Pharmac. J. 27, 1164–1173.
Jubeen, F., Liaqat, A., Amjad, F., et al, 2020. Synthesis of 5-fluorouracil cocrystals with novel organic acids as coformers and anticancer evaluation against HCT-116 colorectal cell lines. Cryst. Growth Des. 20, 2406–2414.
Júnior, Z.S.S., Botta, S.B., Ana, P.A., et al, 2015. Effect of papain-based gel on type I collagen-spectroscopy applied for microstructural analysis. Sci. Rep. 5, 1–7.
Kamble, V., Gaikwad, N., 2016. Fourier Transform infrared spectroscopy spectroscopic studies in embelia ribes burm. F.: a vulnerable medicinal plant. Asian J. Pharm. Clin. Res. 9, 41–47.
Khalafallah, A., Ahmed, M., 2017. A novel and efficient method for the synthesis of 6-amino-pyrimidine-2 (1H)-thiones derivatives, pyrido [2, 3-d] pyrimidine-2 (1H)-thiones derivatives and their glycosides. Chem. Int. 3, 469–476.
Koparir, P., Parlak, A.E., Karatepe, A., et al, 2022. Elucidation of potential anticancer, antioxidant and antimicrobial properties of some new triazole compounds bearing pyridine-4-yl moiety and cyclobutane ring. Arab. J. Chem. 15, 103957.
Kousar, N., Ali, S., Shahzadi, S., et al, 2015. Synthesis, characterization and antimicrobial activities of organotin (IV) complexes with ethylthioglycolate. Chem. Int. 1, 92–98.
Krishnaiah, Y., Satyanarayana, V., Kumar, B.D., et al, 2003. In vivo pharmacokinetics in human volunteers: oral administered guar gum-based colon-targeted 5-fluorouracil tablets. Eur. J. Pharm. Sci. 19, 355–362.
Kristoffersen, K.A., van Amerongen, A., Böcker, U., et al, 2020. Fourier-transform infrared spectroscopy for monitoring proteolytic reactions using dry-films treated with trifluoroacetic acid. Sci. Rep. 10, 1–10.
Kumar, S.U., Gopinath, P., Negi, Y.S., 2017. Synthesis and bio-evaluation of xylan-5-fluorouracil-1-acetic acid conjugates as pro-drugs for colon cancer treatment. Carbohydr. Polym. 157, 1442–1450.
Lang, D.K., Kaur, R., Arora, R., et al, 2020. Nitrogen-containing heterocycles as anticancer agents: An overview. Anti-Cancer Agents Med. Chem. (Form. Curr. Med. Chem.-Anti-Cancer Agents) 20, 2150–2168.
Li, G., Huang, Y., Feng, Q., et al, 2014a. Tryptophan as a probe to study the anticancer mechanism of action and specificity of α-helical anticancer peptides. Molecules 19, 12224–12241.
Li, M., Liang, Z., Sun, X., et al, 2014b. A polymeric prodrug of 5-fluorouracil-1-acetic acid using a multi-hydroxyl polyethylene glycol derivative as the drug carrier. PLoS ONE 9, e112888.
Moisescu-Goia, C., Muresan-Pop, M., Simon, V., 2017. New solid state forms of antineoplastic 5-fluorouracil with anthelmintic piperazine. J. Mol. Struct. 1150, 37–43.
Nadzri, N.I., Sabri, N.H., Lee, V.S., et al, 2016. 5-fluorouracil co-crystals and their potential anti-cancer activities calculated by molecular docking studies. J. Chem. Crystallogr. 46, 144–154.
Niedzwiecki, D., Hasson, R.M., Lenz, H.J., et al, 2017. A study of thymidylate synthase expression as a biomarker for resectable colon cancer: alliance (cancer and leukemia group B) 9581 and 89803. Oncologist 22, 107–114.
Ocheni, A., Clement, U., 2017. Synthesis, characterization and antimicrobial activities of 1, 5-dimethyl-2-phenyl-4-(pyrolidin-2-ylideneamino)-pyrazolidin-3-one and complex with iron (II). Chem. Int. 3, 244–249.
Patil, S.B., Inamdar, S.Z., Das, K.K., et al, 2020a. Tailor-made electrically-responsive poly (acrylamide)-graft-pullulan copolymer based transdermal drug delivery systems: synthesis, characterization, in-vitro and ex-vivo evaluation. J. Drug Delivery Sci. Technol. 56, 101525.
Patil, S.B., Inamdar, S.Z., Reddy, K.R., et al, 2020b. Functionally tailored electro-sensitive poly (acrylamide)-g-pectin copolymer hydrogel for transdermal drug delivery application: synthesis, characterization, in-vitro and ex-vivo evaluation. Drug Delivery Lett. 10, 185–196.
Pérez-Mellor, A., Zehnacker, A., 2017. Vibrational circular dichroism of a 2, 5-diketopiperazine (DKP) peptide: Evidence for dimer formation in cyclo LL or LD diphenylalanine in the solid state. Chirality 29, 89–96.
Petaccia, M., Condello, M., Giansanti, L., et al, 2016. Correction: Inclusion of new 5-fluorouracil amphiphilic derivatives in liposome formulation for cancer treatment. MedChemComm 7. 378-378.
Phan, J., Koli, S., Minor, W., et al, 2001. Human thymidylate synthase is in the closed conformation when complexed with dUMP and raltitrexed, an antifolate drug. Biochemistry 40, 1897–1902.
Pokorna, A., Bobal, P., Oravec, M., et al, 2019. Investigation of permeation of theophylline through skin using selected piperazine-2, 5-diones. Molecules 24, 566.
Prabha, N., Sannasimuthu, A., Kumaresan, V., et al, 2020. Intensifying the anticancer potential of cationic peptide derived from serine threonine protein kinase of teleost by tagging with oligo tryptophan. Int. J. Pept. Res. Ther. 26, 75–83.
Pradhan, A., Vishwakarma, S., 2020. Synthesis of quinolone derivatives and their molecular docking for antiepileptic activity. Chem. Int. 6, 224–231.
Radwan, A.A., Alanazi, F.K., 2014. Design and synthesis of new cholesterol-conjugated 5-fluorouracil: a novel potential delivery system for cancer treatment. Molecules 19, 13177–13187.
Raveesha, R., Anusuya, A.M., Raghu, A.V., et al, 2022. Synthesis and characterization of novel thiazole derivatives as potential anticancer agents: Molecular docking and DFT studies. Comput. Toxicol. 21, 100202.

Richner, G., Puxty, G., 2012. Assessing the chemical speciation during CO2 absorption by aqueous amines using in situ FTIR. Ind. Eng. Chem. Res. 51, 14317–14324.

Sammak, S., Hamdani, N., Gorrec, F., et al, 2019. Crystal structures and nuclear magnetic resonance studies of the Apo form of the c-MYC: MAX bHLHZip complex reveal a helical basic region in the absence of DNA. Biochemistry 58, 3144–3154.

Sanduja, M., Gupta, J., Virmani, T., 2020. Recent advancements in Uracil and 5-Fluorouracil hybrids as potential anticancer agents: A review. J. Appl. Pharmac. Sci. 10, 129–146.

Sethy, C., Kundu, C.N., 2021. 5-Fluorouracil (5-FU) resistance and the new strategy to enhance the sensitivity against cancer: Implication of DNA repair inhibition. Biomed. Pharmacother. 137, 111285.

Shinde, G., Shiyani, S., Shelke, S., et al, 2020. Enhanced brain targeting efficiency using 5-FU (fluorouracil) lipid–drug conjugated nanoparticles in brain cancer therapy. Prog. Biomater. 9, 259–275.

Stoler, E., Warner, J.C., 2015. Non-covalent derivatives: cocrystals and eutectics. Molecules 20, 14833–14848.

Strippoli, A., Cocomazzi, A., Basso, M., et al, 2020. c-MYC expression is a possible keystone in the colorectal cancer resistance to EGFR inhibitors. Cancers 12, 638.

Su, P., Ahmad, B., Zou, K., et al, 2020. β-Elemene enhances the chemotherapeutic effect of 5-fluorouracil in triple-negative breast cancer via PI3K/AKT, RAF-MEK-ErK, and NF-κB signaling pathways. OncoTargets Therapy 13, 5207.

Verdonk, M.L., Cole, J.C., Hartshorn, M.J., et al, 2003. Improved protein–ligand docking using GOLD. Proteins: Structure. Funct. Bioinform. 52, 609–623.

Vidyavathi, G.T., Kumar, B.V., Raghu, A.V., et al, 2022. Punica granatum pericarp extract catalyzed green chemistry approach for synthesizing novel ligand and its metal(II) complexes: Molecular docking/DNA interactions. J. Mol. Struct. 1249, 131656.

Vodenkova, S., Buchler, T., Cervena, K., et al, 2020. 5-fluorouracil and other fluoropyrimidines in colorectal cancer: Past, present and future. Pharmacol. Ther. 206, 107447.

Yan, X., Hou, Y., Chen, F., et al, 2009. Synthesis and structure–antitumor activity relationship of sulfonyl 5-fluorouracil derivatives. Phosphorus Sulfur Silicon 185, 158–164.

Zhang, X., Rakesh, K., Shantharam, C., et al, 2018. Podophyllotoxin derivatives as an excellent anticancer aspirant for future chemotherapy: a key current imminent needs. Bioorg. Med. Chem. 26, 340–355.

Zhou, G., Marathe, G.K., Hartiala, J., et al, 2013. Aspirin hydrolysis in plasma is a variable function of butyrylcholinesterase and platelet-activating factor acetylhydrolase 1b2 (PAFAH1b2). J. Biol. Chem. 288, 11940–11948.

Zhou, Q., Sun, X., Pasquier, N., et al, 2021. Cell-penetrating CEBPB and CEBPD leucine zipper decoys as broadly acting anti-cancer agents. Cancers 13, 2504.